

01 Sep 2019

## Influence of Guayule Resin as a Bio-Based Additive on Asphalt-Rubber Binder at Elevated Temperatures

Ahmed Hemida

Magdy Abdelrahman

*Missouri University of Science and Technology*, [abdelrahmanm@mst.edu](mailto:abdelrahmanm@mst.edu)

Follow this and additional works at: [https://scholarsmine.mst.edu/civarc\\_enveng\\_facwork](https://scholarsmine.mst.edu/civarc_enveng_facwork)



Part of the [Structural Engineering Commons](#)

### Recommended Citation

A. Hemida and M. Abdelrahman, "Influence of Guayule Resin as a Bio-Based Additive on Asphalt-Rubber Binder at Elevated Temperatures," *Recycling*, vol. 4, no. 3, MDPI, Sep 2019.

The definitive version is available at <https://doi.org/10.3390/recycling4030038>



This work is licensed under a [Creative Commons Attribution 4.0 License](#).

This Article - Journal is brought to you for free and open access by Scholars' Mine. It has been accepted for inclusion in Civil, Architectural and Environmental Engineering Faculty Research & Creative Works by an authorized administrator of Scholars' Mine. This work is protected by U. S. Copyright Law. Unauthorized use including reproduction for redistribution requires the permission of the copyright holder. For more information, please contact [scholarsmine@mst.edu](mailto:scholarsmine@mst.edu).

Article

# Influence of Guayule Resin as a Bio-Based Additive on Asphalt–Rubber Binder at Elevated Temperatures

Ahmed Hemida <sup>1,\*</sup>  and Magdy Abdelrahman <sup>2</sup>

<sup>1</sup> Department of Civil, Architectural, and Environmental Engineering, Missouri University of Science and Technology (Missouri S&T), Laura, MO 65409, USA

<sup>2</sup> Missouri Asphalt Pavement Association (MAPA) Endowed Professor; Department of Civil, Architectural, and Environmental Engineering, Missouri University of Science and Technology (Missouri S&T), Laura, MO 65409, USA

\* Correspondence: amhbnc@mst.edu; Tel.: +1-(314)-309-6952

Received: 23 July 2019; Accepted: 3 September 2019; Published: 5 September 2019



**Abstract:** This study seeks to find the influence of replacing a portion of the asphalt–rubber binder with the bio-based material “guayule resin.” This replacement could be beneficial in terms of sustainability, economics, and environmental concerns related to the asphalt industry. Nine asphalt–rubber–guayule binders were investigated to find their rheological properties. Consecutively, the study proceeded with five selected binders being compared to the original asphalt (PG64-22). Investigations underwent whole matrices (crumb rubber modifier (CRM) residue included) and liquid phases (CRM residue extracted). Additionally, these properties were partially sought for their corresponding asphalt–rubber binders to compare and judge the contribution of the guayule resin. Likewise, a thermo-gravimetric analysis was done for the guayule resin to recognize its moisture and composition complexity. Such an analysis was also done for the as-received CRM and some extracted CRMs to determine the release and residue of rubber components. Outcomes showed that the guayule resin has the potential to compensate the performance required against the original asphalt at elevated temperatures while greatly decreasing the asphalt cement proportion. For instance, a blend of 62.5% asphalt, 12.5% CRM, and 25% guayule resin provided better performance than that of the original asphalt.

**Keywords:** asphalt–rubber; BGR; bio-based; CRM; CRMA; guayule; master curve; modified asphalt; interrupted shear flow; TGA

## 1. Introduction

### 1.1. Overview

One of the guayule plant derivatives is guayule resin, which represents a by-product. This by-product is inevitably extracted during guayule natural rubber production as a by-product [1]. Each one kilogram of the produced rubber, at the very least, corresponds to one kilogram of resin [2]. The current value of guayule resin is almost nothing. Some researchers see that about 25–50% savings in the guayule rubber production could be attributed to the exploitation of other associated by-products such as resin, bagasse, wax, seed, and leaves [3].

Guayule resin is composed of volatile (3–5%) and non-volatile fractions (85–97%) [1,4,5]. In other words, it consists of complex mixtures of terpenes, fatty acid triglycerides, and sesquiterpenes [1,4,6,7]. Even though some of these components are volatile, they may have a high boiling point, such as terpenes [8]. In addition, because of the solvent-based extraction process of guayule resin, a significant amount of low-molecular-weight guayule rubber (5000–10,000) is inevitably included in the extracted resin [6]. Further details related to the guayule resin chemical characterization could be found in *Guayule Future Development* by Nakayama [1].

The utilization of guayule resin in the asphalt industry could be beneficial for both guayule commercial value and such a heavy flexible pavement industry. Previously, guayule resin was investigated by the same research group, and the writers observed that guayule resin is an asphalt-like material. It was very susceptible to temperature change—viscoelastic at room temperature, viscous at high temperatures, and solid at low temperatures. Likewise, pure guayule resin provided rheological properties comparable to the original asphalt at specific grades [9]. It could be distinct in the asphalt industry in regard to sustainability and economics as it is a bio-based material and a by-product, respectively [1].

### 1.2. Guayule Resin vs. Asphalt Economics

In 1991, researchers studied the economics of guayule derivative production. Even though this is an old reference [10], it could give indications regarding pricing. For the irrigated conditions, this study reported that at that time the net cost was \$1.21/kg for rubber and \$0.44/kg for resin plus low-molecular-weight rubber [10]. These values change upon interest and inflation values. The average asphalt cement price, at that time, was about \$120/ton (\$0.12/kg) [11]. Nevertheless, the gradual increase in asphalt binder cost is very sharp due to the rapid increase in the international price of crude oil as a nonrenewable source of energy [12]. For instance, around 2009, the asphalt cement underwent an unprecedented price increase to about \$900/ton [11]. However, it decreased to about \$600/ton by 2013. By 2019, it had reached a price of about \$550/ton [13].

### 1.3. Guayule as a Binder Additive

The same research group studied guayule resin in 2018 in *A Threshold to Utilize Guayule Resin as a New Binder in Flexible Pavement Industry* [9]. This study partially discussed the potential of guayule resin as a new additive to the asphalt–rubber (AR) binder as a whole matrix (i.e., including the particle effect) [9]. The particle effect indicates the effect of residual crumb rubber modifier (CRM) particles after the interaction on the overall binder matrix; however, the interaction effect denotes the influence of the dissolved CRM in the binder liquid phase [14]. The current research discusses the effect of CRM extraction from the asphalt–rubber–guayule binder on the resultant liquid phase, specifically the elevated temperature compared to the binder whole matrix. This latter point was investigated in comparison with the original asphalt (PG64-22), in addition to the corresponding asphalt–rubber binders, including the same CRM concentration and interaction speed, time, and temperature.

### 1.4. CRM as an Asphalt Modifier

In this research, the authors pursued the use of guayule resin for a partial asphalt replacement. Nevertheless, since the used asphalt had a higher grade than the guayule resin, as is discussed later, the CRM was used to balance that minimization of behavior, thus triggering a created binder that at least compensated the original asphalt. The tire rubber or the so-called crumb rubber modifier (CRM) worked as an enhancer to the asphalt binder, as proven in literature [15]. Recent studies in this regard have focused on the effect of material parameters (asphalt type, as well as CRM type and size) and interaction parameters (temperature, speed, and time). Some researches declared that temperature is the main interaction parameter affecting the CRM dissolution in asphalt–rubber binders [16,17]. A 190 °C interaction temperature has the potential to develop the liquid phase of the asphalt rubber binder [16,17]. Besides, a 3000 rpm interaction speed has the potential to result in a more homogenous asphalt–rubber binder [16,17]. The CRM was difficult to entirely dissolve in asphalt due to its cross-linked structure [18]. Nevertheless, the above-mentioned specific interaction parameters were proven to be attributed to the formation of a 3D network structure, which was significantly effective in terms of the binder rheological properties enhancement [19]. Consecutively, the authors in this research followed the same interaction temperature and speed for the created binders, as is discussed later.

### 1.5. Significance of Studying Whole Matrix and Liquid Phase

As mentioned above, the CRM has two effects on asphalt modification. One of them is the liquid phase, which corresponds to the interaction effect, meaning no effect of the CRM particle (residue) on the binder's performance. The other one is the whole matrix, which involves the particle effect involving the dispersed CRM residue in the binder's matrix performance. Previous studies have depicted a relatively higher performance attributed to the whole matrix [20]. It was essential to study the effects of both products on performance. In this research, the impact of the guayule resin as a new bio-based additive on the asphalt-rubber was studied on the two scales (whole matrix and liquid phase).

### 1.6. Objective

The main objective was to partially replace the original asphalt (PG64) rheological behavior at elevated temperatures using guayule resin (PG52) as a new bio-based additive and a CRM as an enhancer. Per blend component concentrations, the asphalt-rubber-guayule binders were investigated with asphalt concentrations from 22.7–62.5%, CRM concentrations from 2.3–12.5%, and guayule concentrations from 25–75%. Upon which, this replacement could be beneficial in terms of sustainability, economics, and environmental concerns related to the asphalt industry. In order to judge the contribution of guayule resin, selected asphalt-rubber-guayule binders were compared to their corresponding asphalt-rubber binders. In order to judge the contribution of the CRM, binder whole matrices and liquid phases were investigated as the CRM was partially dissolved in the blend.

## 2. Experimental Plan

Binder blends were created from asphalt, rubber, and guayule resin. The original asphalt had a PG64-22 (source: Philips 66 Company, Granite City, IL, USA). The source of the CRM was Liberty Tire Recycling LLC. Different sizes of CRM were obtained. However, it was sieved, and the selected gradation was the so-called CRM 30–40 (passing sieve #30 and remaining on sieve #40) according to the US standard system [11,21,22]. Guayule resin was provided by Bridgestone Americas, Mesa, AZ, USA (abbreviated to "BGR") and produced from a mix of three different batches (2016-7-1-RES-12, -13, and -14).

This study involved three major groups of interactions among asphalt, rubber, and guayule resin, as follows: (1) 25% AR + 75% BGR, (2) 50% AR + 50% BGR, and (3) 75% AR + 25% BGR. Each group of those included three subgroups. For example, 25% AR + 75% BGR contained 25% of the asphalt-rubber binder plus 75% of the guayule resin (by wt. of blend). However, the 25% AR was divided into three subcategories, as follows: (1-a) 10% CRM, (1-b) 15% CRM, and (1-c) 20% CRM (by wt. of asphalt cement (AC)). As is justified hereafter, five of the nine asphalt-rubber-guayule binders were selected to proceed in the upcoming discussion, and these were AR-BGR25-10, AR-BGR50-15, AR-BGR50-20, AR-BGR75-10, and AR-BGR75-20, as described in Table 1. Thus, these selected binders were physically compared to their corresponding asphalt-rubber binders to investigate how much asphalt-rubber-guayule binders contribute while taking into account that the guayule resin had a PG52 and the original asphalt had a PG64. Therefore, adding guayule resin to the asphalt-rubber binder would likely negatively affect the physical properties of the final product upon the different proportions of asphalt, rubber, and guayule resin. These asphalt-rubber binders were AR25-10 (AC + 2.3% CRM), AR50-15 (AC + 6.5% CRM), AR50-20 (AC + 8.3% CRM), AR75-10 (AC + 6.8% CRM), and AR75-20 (AC + 12.5% CRM). The flowchart of materials is illustrated in Figure 1a. In order to compare the asphalt-rubber-guayule binders and asphalt-rubber binders, physical tests were implemented and represented by the elevated-temperature grade in terms of whole matrices and liquid phases. Table 1 defines the names of groups and subgroups/codes that may be used to describe the designated binders in this research. Table 1 also lists the detailed concentrations of binder materials.

**Table 1.** Experimental groups, subgroups, coding, and detailed proportions.

Group	Subgroup/Code	Binder Proportions				
		AR% by wt. of Blend	BGR% by wt. of Blend	CRM% by wt. of AC	CRM% by wt. of Blend	AC% by wt. of Blend
25% AR + 75% BGR	AR-BGR25-10 <sup>1</sup>	25	75	10	2.3	22.7
	AR-BGR25-15 <sup>1</sup>	25	75	15	3.3	21.7
	AR-BGR25-20 <sup>1</sup>	25	75	20	4.2	20.8
	AR25-10 <sup>2</sup>	100	0	2.4	2.3	97.7
50% AR + 50% BGR	AR-BGR50-10 <sup>1</sup>	50	50	10	4.5	45.5
	AR-BGR50-15 <sup>1</sup>	50	50	15	6.5	43.5
	AR-BGR50-20 <sup>1</sup>	50	50	20	8.3	41.7
	AR50-15 <sup>2</sup>	100	0	7	6.5	93.5
	AR50-20 <sup>2</sup>	100	0	9.1	8.3	91.7
75% AR + 25% BGR	AR-BGR75-10 <sup>1</sup>	75	25	10	6.8	68.2
	AR-BGR75-15 <sup>1</sup>	75	25	15	9.8	65.2
	AR-BGR75-20 <sup>1</sup>	75	25	20	12.5	62.5
	AR75-10 <sup>2</sup>	100	0	7.3	6.8	93.2
	AR75-20 <sup>2</sup>	100	0	14.3	12.5	87.5

<sup>1</sup> e.g., AR-BGR25-10 represents 25% of asphalt-rubber (AR) binder (including 10%CRM by wt. of asphalt cement (AC) and 75% of guayule resin (BGR)). <sup>2</sup> However, AR25-10 represents its corresponding asphalt-rubber binder (i.e., the same CRM concentration and interaction speed, time, and temperature). Both AR-BGR25-10 and AR25-10 contained 2.3% CRM by wt. of (all) blend.

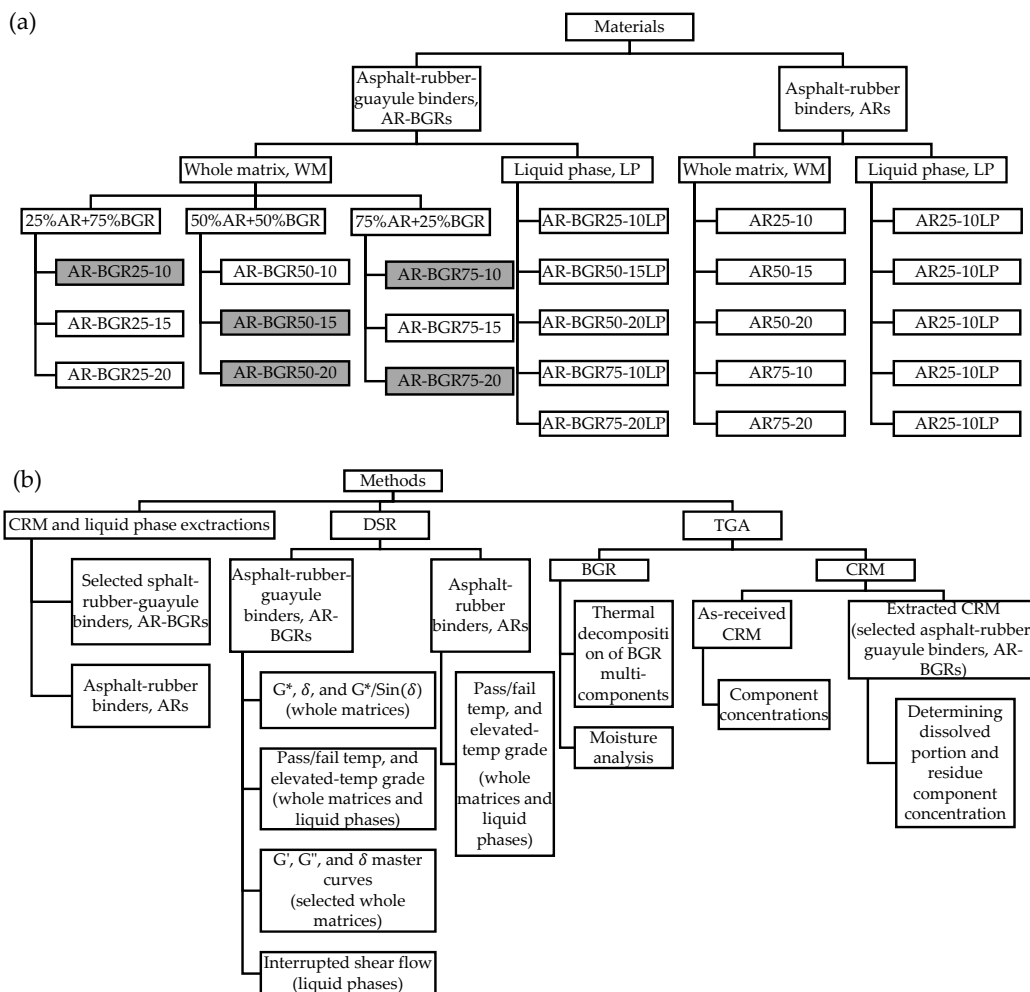


**Figure 1.** Flowcharts of experimental plan: (a) Materials and (b) methods. The five selected asphalt-rubber-guayule binders for the study completion are highlighted in (a).

## 2.1. Mixing Process

The mixing technique was applied, as recommended in the literature [23–25]. The HSM100LCIT high shear mixer was used for mixing. Furthermore, a heating system was employed to control the binder temperature during the mixing process, which included the 100C M112 Glas-Col mantle and the TC9100 Digi-Sense controller.

## 2.2. Sampling

### 2.2.1. Asphalt–Rubber–Guayule Binder

Each quart can was filled with 750 g of preheated asphalt cement. An oven-dried CRM was added as a proportion of asphalt cement. The asphalt–rubber portion was mixed for 40 min interaction time at a 190 °C interaction temperature and a 3000 rpm interaction speed. About 680 g of the asphalt–rubber binder was distributed in three cans with respect to the design proportions (113.4, 226.7, and 340 g, a can for each asphalt–rubber–guayule mix). This process was repeated three times, one for each CRM concentration (10%, 15%, and 20% by wt. of AC). The extra amount was lost between the transfer losses and dynamic shear rheometer (DSR) specimens that were withdrawn during and after the mixing process.

The guayule resin was heat-treated for 4 h at 160 °C and 600 rpm (labeled B(4)) to ensure that no moisture was inside during the so-called heat-treatment process. DSR specimens were withdrawn at 0, 120, and 240 min to monitor the material's rheological behavior change. This process was replicated three times. Each replication included 700 g of guayule resin in a quart can distributed in three cans containing the asphalt–rubber portion (25%, 50%, and 75%), as mentioned above. As such, the guayule resin was poured in concentrations of 75%, 50%, and 25%. Each blend of the asphalt–rubber–guayule binder was mixed for 60 min at 160 °C and 600 rpm as a final step for material preparation ending with nine cans, each one with different asphalt, rubber, and guayule resin concentrations.

### 2.2.2. Asphalt–Rubber Binder

The asphalt–rubber binders were created to correspond to the five selected asphalt–rubber–guayule binders. That is why they were prepared using the same approach as explained above, except for diluting the asphalt–rubber portion with extra asphalt instead of guayule resin to end up with the same CRM concentration and same interaction speed, time, and temperature.

## 2.3. Methods

The attributed methods are listed in the “methods” flowchart, Figure 1b, and interpreted in details in the following sections.

### 2.3.1. CRM and Liquid Phase Extractions, Solubility, and Phase Separation

The CRM and liquid phase extractions were implemented for the five selected asphalt–rubber–guayule binders and their corresponding asphalt–rubber binders with respect to the methodology of previous researchers, as interpreted in the following two bullets [11].

- CRM Extraction Stepwise
  1.  $10 \pm 2$  g of modified asphalt is diluted in 100 g of trichloroethylene for 25 min.
  2. The modified asphalt solution passes through mesh #200 (75  $\mu$ m).
  3. Retained CRM particles are washed with extra trichloroethylene until the filtrate becomes colorless.
  4. Washed CRM particles are kept in an oven at 60 °C for 12 h to ensure a complete solvent removal.
- Liquid Phase Extraction Stepwise
  1. The required amount of the binder is heated to 165 °C.
  2. That heated binder is drained through mesh #200 (75  $\mu$ m) in the oven at 165 °C for 25 min.

3. Extracted liquid phase is stored at  $-12\text{ }^{\circ}\text{C}$  immediately to prevent any unwanted aging or reaction.

Regarding the new additive (guayule resin), the solubility test was applied according to ASTM D2042/AASHTO T44 [26,27]. Likewise, the same test was implemented for a blend of asphalt and guayule resin. This test could indicate whether lumps of guayule resin were retained. In order to conduct this test, the asphalt–guayule blend was prepared with proportions of 50:50, mixed at 3000 rpm and  $190\text{ }^{\circ}\text{C}$  for 2 h. This basic solubility test resulted in almost 100% solubility, either for pure guayule resin in trichloroethylene or the asphalt–guayule blend in trichloroethylene, and no attributed coagulation was noticed. Since this test might not have been entirely representative regarding the guayule resin solubility in asphalt and an issue might still be there regarding the asphalt–guayule compatibility, the separation tendency test, according to ASTM D7173 [28], was implemented for the same asphalt–guayule blend. This test aimed to investigate the asphalt–guayule phase separation as interpreted by the separation index (SI) in Equation (1), [29].

$$SI = \frac{\text{Max}(G^*_{\text{top}}, G^*_{\text{bottom}}) - G^*_{\text{avg}}}{G^*_{\text{avg}}} \times 100, \quad (1)$$

In Equation (1),  $G^*_{\text{top}}$  represents the complex modulus of the top portion,  $G^*_{\text{bottom}}$  represents the complex modulus of the bottom portion, and  $G^*_{\text{avg}}$  represents the average complex modulus of the top and bottom portions. This test resulted in an SI of 1.53% after exposing the blend to a  $163\text{ }^{\circ}\text{C}$  temperature for 48 h in a cigar tube, indicating almost no asphalt–guayule phase separation. Accordingly, the potential of high compatibility between asphalt and guayule existed. It was believed by many researchers that there is a strong relationship between compatibility and solubility [30–34]. As a result, one could say that the guayule resin had the potential to be soluble in asphalt.

### 2.3.2. Dynamic Shear Rheometer (DSR)

An Anton Paar MCR302 DSR was employed, according to AASHTO T315 [35], to investigate the rheological properties (complex shear modulus ( $G^*$ ) and phase angle ( $\delta$ )) in addition to the rutting parameter ( $G^*/\text{Sin}(\delta)$ ). Consequently, the pass/fail (elevated) temperature and the elevated-temperature grade were determined. All of these rheological properties were investigated for all asphalt–rubber–guayule binders. In addition to asphalt–rubber–guayule binders, their corresponding asphalt–rubber binders were compared regarding high-temperature grading on the two scales (whole matrix and liquid phase).

As binder grading may not be sufficient to evaluate binder performance, since it is controlled by specific parameters such as a frequency of 10 rad/s, the master curve is an excellent tool to show the effect of wide ranges of frequencies and temperatures on the binder behavior. Subsequently, the frequency sweep test was applied at multiple temperatures to build up the master curves of selected binders (AR-BGR25-10, AR-BGR50-15, AR-BGR50-20, AR-BGR75-10, and AR-BGR75-20) in order to study their behaviors under the loading rate change. Master curves were investigated in terms of the storage modulus ( $G'$ ), loss modulus ( $G''$ ), and phase angle ( $\delta$ ).

The interrupted shear flow test was applied for all asphalt–rubber–guayule liquid phases. Previous researchers studied the formation of a 3D network structure [19,29,36,37]. Those references [19,29,36,37] declared the 3D network structure formation indicates higher performance of the binder than that of no apparent 3D network structure formation. Regarding the rheological analysis limitations, this was evident by the creation of a peak overshoot of shear stress with the application kickoff; hence, steady-state shear flow with time was clarified by Ragab et al. (2013), and Ragab and Abdelrahman (2018) [19,29]. In this research, this test was started at a temperature of  $64\text{ }^{\circ}\text{C}$  after a waiting time of 30 min and was attributed to a shear rate of  $2\text{ s}^{-1}$  [19,29,36,37], under the strain control regime [36,37]. The initial stress growth was applied for 60 s and then applied again (second stress growth) for the same duration [36] after the rest time to follow its development and trend up to recovery. Upon multiple experimental trials, the rest time was selected to be 5, 10, 20, 30, 40 and 50 s, as the required information for analysis was obtained through this range which was a

rapid time for binder's full recovery compared to literature, as is interpreted later. One continuous test was conducted for each binder sample with a rest time of 5 min since this was more than enough to ensure getting the original sample state with the second stress growth [29].

The gap between the upper and lower plates was selected to be 2 mm for all binders, including CRM residue, to avoid the effect of particles on the rheological properties [38–40]. However, it was applied 1 mm for all liquid binders [35].

### 2.3.3. Thermo-Gravimetric Analysis (TGA)

A Q50 thermo-gravimetric analyzer, from TA Instruments, was utilized for the compositional analysis of the guayule resin in order to analyze moisture and multi-components included, in addition to the as-received and extracted CRM in order to show the released constituents of the CRM into the binder liquid phase, as utilized by previous researchers in this regard [19,20,22,23,41]. Two methods were employed according to material nature [22]. The first and most common one is the ramp method, which is used to analyze materials containing a distant thermal decomposition of its components. In this method, the sample is heated to a predetermined temperature utilizing a constant heating rate that models the mass loss as a function of temperature [15]. That is why it was used for the TGA of the as-received CRM and the extracted CRM from the selected asphalt–rubber–guayule binders. The other method is called the stepwise isothermal thermo-gravimetric (SITG) method, which is a better TGA approach in the case of the closeness of the decomposition temperatures of a multi-component material [15,22,42]. In this method, the sample is subjected to a programmed heating method to ensure that the distinction of material's decomposition will take place with no overlap. Consequently, it was employed for the TGA of guayule resin, as the ramp method was carried out with no distinctive outcomes. Nevertheless, it was employed as a rapid approach to indicate 100% of material's decomposition to define the decomposition temperature range. In this method, 20–25 mg was analyzed at a 20 °C/min heating rate, starting at room temperature until reaching the resultant full decomposition temperature (450 °C), which is explained hereafter.

For a CRM, an amount of 20–25 mg was analyzed with a 20 °C/min heating rate starting from the ambient temperature and reaching 600 °C. According to literature, a CRM has four major components: Oily components, natural rubber, synthetic rubber, and filler components such as carbon black. Each component has its range of decomposition temperatures. The first region corresponds to the oily components and is from 25 to 300 °C, the second region corresponds to natural rubber and is from 300 °C to the temperature corresponding to the minimum point between the two peaks in the derivative thermo-gravimetric (DTG) curve, and the last region is the filler components at 500 °C [15,22].

## 3. Results and Discussion

### 3.1. Elevated Temperature Tests

Tested binders were categorized into 13 initiated binders, including the original asphalt (AC), unconditioned guayule resin (B(U)), heat-treated guayule resin for 2 h and 4 h (B(2) and B(4), respectively), and the nine categories of asphalt–rubber–guayule binders, all described in Table 2. The  $G^*$ ,  $\delta$ ,  $G^*/\sin(\delta)$ , pass/fail temperature, and elevated-temperature grade were determined for each binder.

With considering the Superpave standard, according to AASHTO T315, the original asphalt had a higher performance than that of the guayule resin, PG64, and PG52, respectively (Table 2). They presented a pass/fail elevated temperature of 65.6 and 57.4 °C, respectively. We noticed that the heat treatment process of guayule resin improved its performance after a 2 h heat treatment. However, a little-to-no change in performance was observed when the heat treatment spent 4 h, indicating a material-consistent manner. The authors saw that this consistent manner was yielded due to the following potentials: (a) Removing moisture, and/or (b) eliminating low molecular weight components. This was further investigated using the TGA. As expected, adding guayule resin to the asphalt–rubber binder resulted in a potential to equilibrate the original asphalt performance.

**Table 2.** Superpave grading of unaged binders at elevated temperatures.

Binder	Binder Code	Temp [°C]	G* [kPa]	$\delta$ [°]	G*/sin( $\delta$ ) [kPa]	Pass/Fail Temp [°C]	Elevated-Temp Grad
Original Asphalt	AC	46	14.8	81	15.0	65.6	64
		52	6.1	83	6.2		
		58	2.7	85	2.7		
		64	1.2	87	1.2		
		70	0.6	88	0.6		
BGR (Unconditioned)	B(U)	46	5.1	85	5.1	55.0	52
		52	1.7	87	1.7		
		58	0.6	87	0.6		
BGR-600-160(2 h) <sup>1</sup>	B(2)	46	8.5	85	8.5	57.2	52
		52	2.5	87	2.5		
		58	0.9	87	0.9		
BGR-600-160(4 h) <sup>1</sup>	B(4)	46	9.4	85	9.5	57.4	52
		52	2.7	86	2.7		
		58	0.9	87	0.9		
25% AR (10% CRM) + 75% BGR <sup>2</sup>	AR-BGR25-10	46	10.8	84	10.9	59.3	58
		52	3.5	85	3.6		
		58	1.2	87	1.2		
		64	0.5	87	0.5		
50% AR (10% CRM) + 50% BGR <sup>2</sup>	AR-BGR50-10	46	13.1	81	13.3	62.3	58
		52	4.6	84	4.7		
		58	1.8	85	1.8		
		64	0.8	87	0.8		
75% AR (10% CRM) + 25% BGR <sup>2</sup>	AR-BGR75-10	46	18.9	75	19.6	67.0	64
		52	7.5	79	7.7		
		58	3.2	82	3.2		
		64	1.4	85	1.4		
		70	0.7	86	0.7		
25% AR (15% CRM) + 75% BGR <sup>2</sup>	AR-BGR25-15	46	10.7	82	10.8	60.2	58
		52	3.7	84	3.7		
		58	1.4	86	1.4		
		64	0.6	87	0.6		
50% AR (15% CRM) + 50% BGR <sup>2</sup>	AR-BGR50-15	46	14.4	78	14.7	64.0	64
		52	5.4	80	5.5		
		58	2.2	82	2.2		
		64	1.0	84	1.0		
		70	0.5	85	0.5		
75% AR (15% CRM) + 25% BGR <sup>2</sup>	AR-BGR75-15	46	23.0	70	24.6	70.9	70
		52	10.0	72	10.5		
		58	4.6	76	4.7		
		64	2.2	79	2.2		
		70	1.1	82	1.1		
		76	0.6	84	0.6		
25% AR (20% CRM) + 75% BGR <sup>2</sup>	AR-BGR25-20	46	10.9	82	11.0	61.0	58
		52	3.9	84	4.0		
		58	1.5	85	1.5		
		64	0.6	86	0.6		
50% AR (20% CRM) + 50% BGR <sup>2</sup>	AR-BGR50-20	46	15.0	76	15.5	64.7	64
		52	5.8	79	5.9		
		58	2.4	81	2.4		
		64	1.1	83	1.1		
		70	0.5	85	0.5		
75% AR (20% CRM) + 25% BGR <sup>2</sup>	AR-BGR75-20	46	22.6	68	24.5	72.2	70
		52	10.3	70	10.9		
		58	4.9	73	5.1		
		64	2.4	77	2.5		
		70	1.2	79	1.3		
		76	0.7	82	0.7		

<sup>1</sup> e.g., BGR-600-160 (2 h) means guayule resin-interaction speed in rpm-interaction temperature in °C (interaction time in hr), labeled B(2). <sup>2</sup> e.g., 25% AR (10% CRM) + 75% BGR means 25% of asphalt-rubber binder (including 10% of CRM by wt. of AC) and 75% of guayule resin, labeled AR25-10. (e.g., AR-BGR50-15, AR-BGR50-20, AR-BGR75-10, and AR-BGR75-20), but others such as AR-BGR25-10 resulted in performance away from achieving that of the original asphalt. One may observe that the higher the asphalt-rubber concentration, the higher the G\* values and the lower the  $\delta$  value at a specific temperature.

### 3.2. Proceeding with Selected Asphalt–Rubber–Guayule Binders and Asphalt–Rubber Binders

Five of the nine asphalt–rubber–guayule binders have the potential to proceed in the upcoming discussion, and they are tabulated with justification for selection in Table 3. The following sections consider the liquid phase vs. the whole matrix for not only the five selected asphalt–rubber–guayule binders but also their corresponding asphalt–rubber binders.

**Table 3.** Selected binders attributed to the justification for selection.

Binder	Binder Code	Justification for Selection (Upon Study Limitations)
75% AR (10% CRM) + 25% BGR	AR-BGR75-10	Low concentrations of CRM (10% by wt. of AC) and guayule resin (25% by wt. of blend) that could significantly achieve the same high grade of the original asphalt.
50% AR (20% CRM) + 50% BGR	AR-BGR50-20	High CRM concentration (20%) and average guayule resin concentration, 50% that could significantly achieve the same grade of the original asphalt.
50% AR (15% CRM) + 50% BGR	AR-BGR50-15	Compared to the last, the CRM was lowered to 15%, the critical requirement (very close to $G^*/\text{Sin}(\delta)$ of 1 kPa at 64 °C) could be accomplished.
25% AR (10% CRM) + 75% BGR	AR-BGR25-10	Low concentrations of CRM (10%) and asphalt (25%) to show results away from achieving that of the original asphalt.
75% AR (20% CRM) + 25% BGR	AR-BGR75-20	Highest concentrations of CRM (20%) and asphalt (75%) that could go beyond the original asphalt performance.

#### 3.2.1. Whole Matrix vs. Liquid Phase Grade Susceptibility

A created term called the liquid phase percentage (LP%) denoted the portion of the liquid phase pass/fail (elevated) temperature relative to the whole matrix pass/fail temperature of a particular binder as a percentage and is defined in Equation (2).

$$\text{LP}\% = \frac{\text{liquid phase pass/fail temperature}}{\text{whole matrix pass/fail temperature}} \times 100, \quad (2)$$

The LP% was created only to show the interaction effect on the binder liquid phase performance as a function of the pass/fail temperature. As shown in Table 4, the variation between the whole matrix performance grade (PG) and the LP PG was not significant at the elevated temperature, indicating a high contribution of the dissolved CRM. Furthermore, the LP% of AR-BGR25-10 showed an almost identical PG for both whole matrix and liquid phase at the elevated temperature (99.6%), which was justified by the low CRM concentration (2.3% by wt. of blend). However, it was lower for AR-BGR50-15, AR-BGR50-20, and AR-BGR75-10, which were all in the range of 96%–97% relative to the intermediate CRM concentrations of 6.5%, 8.3%, and 6.8%, respectively. On the other hand, when raising the CRM concentration to 12.5% for AR-BGR75-20, the LP% decreased to 93.6%. The LP% of the corresponding asphalt–rubber binders was relatively lower, indicating a lower performance when the asphalt–rubber binder performed as a liquid phase compared to the corresponding liquid phase of the asphalt–rubber–guayule binder. For example, the LP% of AR-BGR25-10 was 99.6% against 98.7% for AR25-10.

**Table 4.** Whole matrix vs. liquid phase grade susceptibility.

Binder	Binder Code	CRM% by wt. of Blend	Whole Matrix		Liquid Phase		LP% <sup>1</sup>
			Pass/Fail Temp [°C]	PG	Pass/Fail Temp [°C]	PG	
25% AR (10% CRM) + 75% BGR	AR-BGR25-10	2.3	59.3	58	59.1	58	99.6
25% AR (10% CRM) + 75% AC	AR25-10	2.3	67.8	64	66.9	64	98.7
50% AR (15% CRM) + 50% BGR	AR-BGR50-15	6.5	64.0	64	61.8	58	96.5
50% AR (15% CRM) + 50% AC	AR50-15	6.5	72.3	70	69.1	64	95.7
50% AR (20% CRM) + 50% BGR	AR-BGR50-20	8.3	64.7	64	62.2	58	96.2
50% AR (20% CRM) + 50% AC	AR50-20	8.3	74.4	70	70.2	70	94.3
75% AR (10% CRM) + 25% BGR	AR-BGR75-10	6.8	67.0	64	64.7	64	96.6
75% AR (10% CRM) + 25% AC	AR75-10	6.8	72.9	70	69.5	64	95.3
75% AR (20% CRM) + 25% BGR	AR-BGR75-20	12.5	72.2	70	67.6	64	93.6
75% AR (20% CRM) +25% AC	AR75-20	12.5	80.5	76	73.5	70	91.3

<sup>1</sup> Applied at a 64 °C elevated temperature.

### 3.2.2. Rutting Parameters: Asphalt–Rubber–Guayule Binders vs. Asphalt–Rubber Binders

Figure 2a,b compares the rutting parameter of asphalt–rubber–guayule binders to the corresponding asphalt–rubber binders and the original asphalt at 64 °C at the two scales (liquid phase and whole matrix). On the liquid phase scale, the dissolved CRM improved the asphalt–rubber–guayule binder physical properties. For instance, the liquid phase of AR-BGR75-20 (labeled AR-BGR75-20LP) had a  $G^*/\sin(\delta)$  of 1.6 kPa, while AR-BGR75-10LP achieved 1.1 kPa. It is known that the CRM significantly improves asphalt–rubber binder physical properties, as shown in Figure 2a,b on the liquid phase scale and whole matrix scale, respectively. According to the study limitations, the so-called AR-BGR/AR ratio, as a function of  $G^*/\sin(\delta)$ , was from 0.4 to 0.6 on the liquid phase scale (derived from Figure 2a). On the whole matrix scale, this latter ratio was 0.3–0.5 (derived from Figure 2b). This meant that the CRM residual particle effect on the asphalt–rubber binder was relatively better than the AR-BGR. On the other hand, all whole matrices of asphalt–rubber–guayule binders (except AR-BGR25-10) performed well against the original asphalt with higher performances occurring with higher asphalt and CRM concentrations. However, in regard to the liquid phases’ investigation, the AR-BGR75-10LP and AR-BGR75-20LP had performances of 1.1 and 1.6 kPa, respectively, which could be compared to the original asphalt.

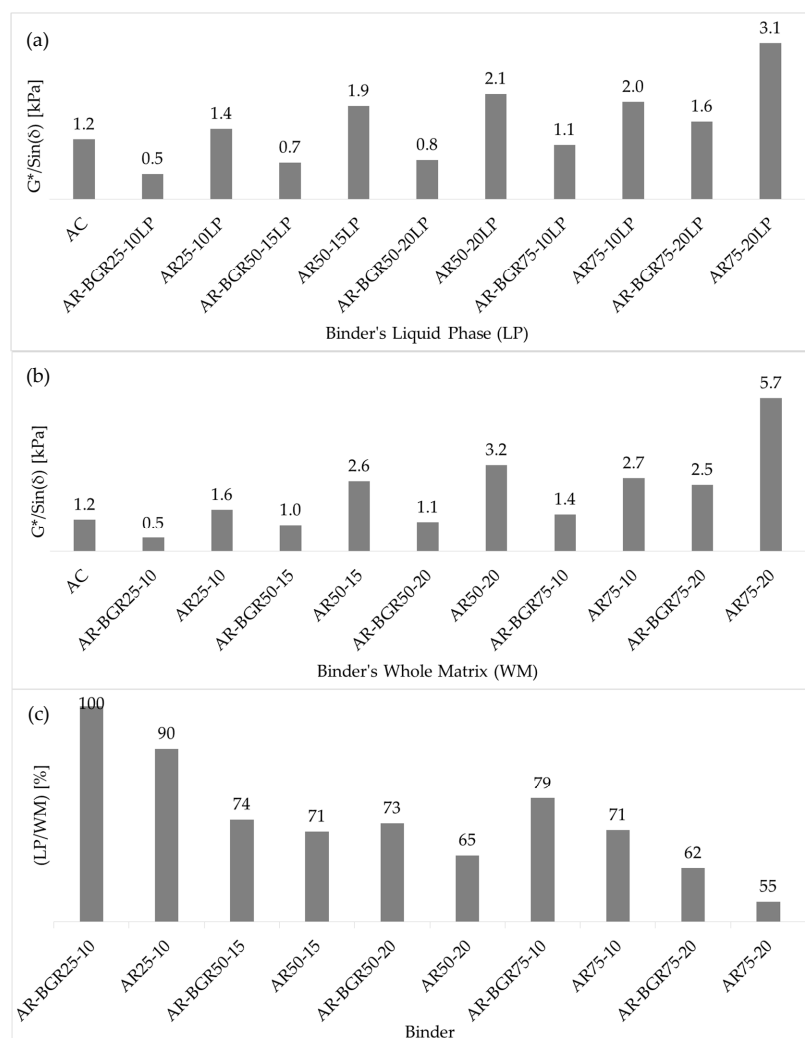


**Figure 2.** Comparing the rutting parameter of the five asphalt–rubber–guayule binders to the corresponding asphalt–rubber binders at 64 °C: (a) liquid phase; (b) whole matrix; (c) percentage of liquid phase per whole matrix (LP/WM%) as a function of complex shear modulus/sin phase angle ( $G^*/\sin(\delta)$ ).

For more clarification, Figure 2c depicts the percentage of liquid phase per the whole matrix (LP/WM%) as a function of  $G^*/\sin(\delta)$ . It was noticed that the effect of removing the residual CRM particles from the binder matrix was relatively better for the asphalt–rubber–guayule binder compared to the asphalt–rubber binder as was also verified by LP%, as shown in Table 4.

### 3.2.3. Master Curves

Master curves of the selected whole matrices (AR-BGR25-10, AR-BGR50-15, AR-BGR50-20, AR-BGR75-10, and AR-BGR75-20), as well as B(4) and AC, are illustrated in Figure 3 with a selection of a 50 °C reference temperature. These master curves showed the effects of the frequency sweep along with temperature sweep on the material rheology represented by  $G'$ ,  $G''$ , and  $\delta$ . In asphalt–rubber–guayule binders, a higher guayule resin concentration significantly affected the master-curve trends due to the different behavior associated with the guayule resin compared to the original asphalt. This different behavior led to an observed thermo-complexity showed by some master curves (Figure 3c) being interpreted hereafter. Overall, the guayule resin provided a better trend at low frequencies. However, the original asphalt provided a better trend at high frequencies.

In terms of  $G'$  and  $G''$ , it was observed that the higher guayule resin-including binders (mentioned here to denote the B(4) and AR-BGR25-10 binders) indicated a higher stiffness at low frequencies, as shown in Figure 3a,b, which developed a plateau investigated in depth in the next section. The higher the asphalt and/or CRM concentrations, the higher the behavior except for the higher guayule resin-including binders at low frequencies. For instance, AR-BGR75-20 presented the best trends except for the distinct B(4) and AR-BGR25-10 at low frequencies. On average, the original asphalt showed a lower sensitivity to frequency and temperature. AR-BGR25-10 provided a guayule-like trend represented by the B(4) trend. Both B(4) and AR-BGR25-10 had lower behaviors than that of the original asphalt at high frequencies and higher behaviors at low frequencies, as mentioned above. Overall, what was distinct for all asphalt–rubber–guayule binders except AR-BGR25-10 was the high behavior at low frequencies, as well as their gradual increase of behaviors with higher frequencies to be close to the original asphalt behavior.

As is shown in Figure 3c, the B(4) and AR-BGR25-10 presented unconventional  $\delta$  trends, which were unlike what the original asphalt presented. In other words, the original asphalt provided a  $\delta$  trend formed higher to lower from low frequencies to high frequencies, respectively, which was contrary to the provided  $\delta$  trend of the higher guayule resin-including binders. Accordingly, the other asphalt–rubber–guayule binders showed a thermo-complexity via their  $\delta$  trends. For instance, the  $\delta$  trend of AR-BGR75-20 started low at 0.001 Hz, reaching its peak at about 0.01 Hz, gradually going down until 10 Hz, and ending up with a horizontal trend. This fluctuation could be analyzed by the influence of the contrary trends of asphalt against guayule resin in terms of the  $\delta$ . Other asphalt–rubber–guayule binders such as AR-BGR50-15 and AR-BGR50-20 presented significantly scattered regimes. Nevertheless, their average trends showed the lowest sensitivity to temperature and frequency than original asphalt. This could be analyzed by balancing the concentrations of asphalt–rubber and guayule resin in the blend.

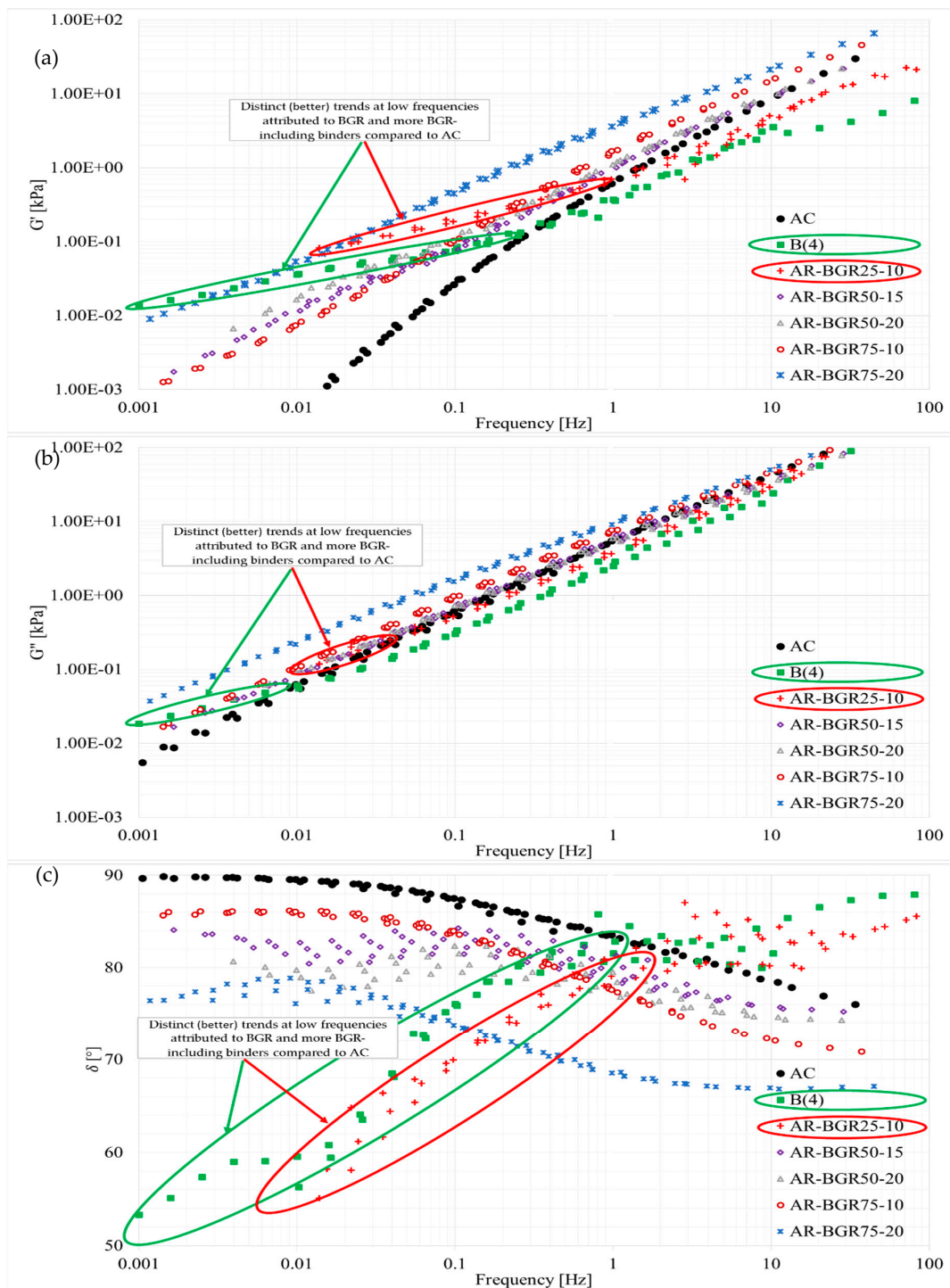


**Figure 3.** Master curves of asphalt–rubber–guayule whole matrices compared to asphalt cement (AC) and 4 h heat-treated guayule resin (B(4)) at a 50 °C reference temperature: (a) storage modulus ( $G'$ ), (b) loss modulus ( $G''$ ), and (c)  $\delta$ .

### 3.2.4. Guayule Resin Privilege

One of the significant problems that face the asphalt binder behavior at high temperatures is the undesired  $\delta$  behavior with traffic speed tolerance. The  $\delta$  is desired to be lower at lower speeds (frequencies) and vice versa. Not only that, but a higher stiffness is also desired at lower frequencies and vice versa. Briefly, the lower the traffic speed, the more the elasticity and stiffness are desired. At this

point, the stiffness resists the traffic load, and the elasticity helps the binder to recover. The guayule resin has the potential of being attracted for the entirely desired  $\delta$  behavior (Figure 3c) and partially desired  $G'$  and  $G''$  behaviors at lower frequencies (Figure 3a,b).

At lower frequencies, the master curves of guayule resin offered an unconventional behavior. Guayule resin presented the best behavior compared to all others at low frequencies for all three major rheological parameters— $G'$ ,  $G''$ , and  $\delta$  (Figure 3). That is why it showed better performance ( $G^*/\sin(\delta)$ ) than that of the original asphalt at low frequencies, as shown in Figure 4. For  $G'$  trends, the guayule resin presented a behavior much better than the original asphalt, while the frequency was lower than 0.3 Hz (e.g., 0.01 and 0.00001 kPa, respectively, at 0.001 Hz). For  $G''$  trends, a similar scenario was observed in which the guayule resin presented better behavior than asphalt while the frequency was lower than 0.01 Hz (e.g., 0.011 and 0.002 kPa, respectively, at 0.001 Hz). As mentioned above, the guayule resin presented an unconventional  $\delta$  trend that was contrary to the original asphalt (Figure 3c). In terms of frequency sweep, this trend is desirable as it yields a higher elastic behavior at low frequencies, unlike the traditional behavior attributed to the original asphalt. Consecutively, the guayule resin presented desirable characteristics at low frequencies since it presented higher  $G'$  and  $G''$ , as well as lower  $\delta$ . This distinction could be beneficial when vehicles stop since the pavement is desired to be stiffer (to resist the loads at low frequencies) and more elastic (to recover when deformed).

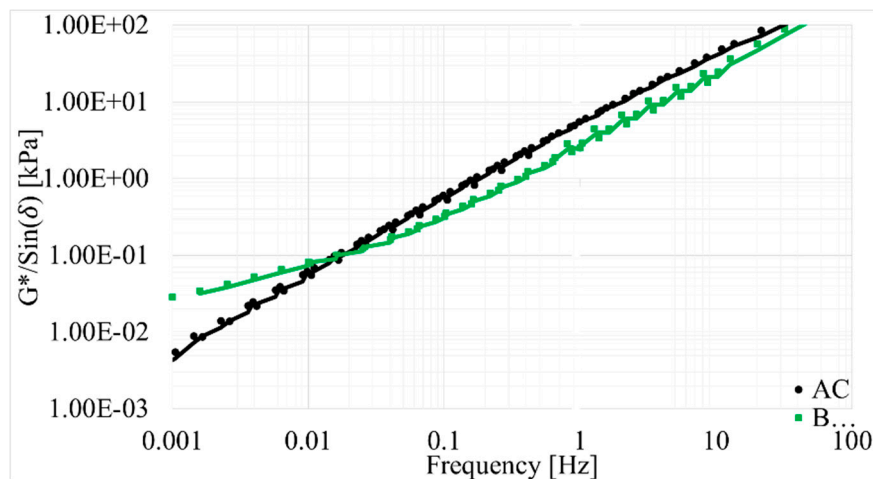


Figure 4.  $G^*/\sin(\delta)$  master curves of guayule resin vs. original asphalt.

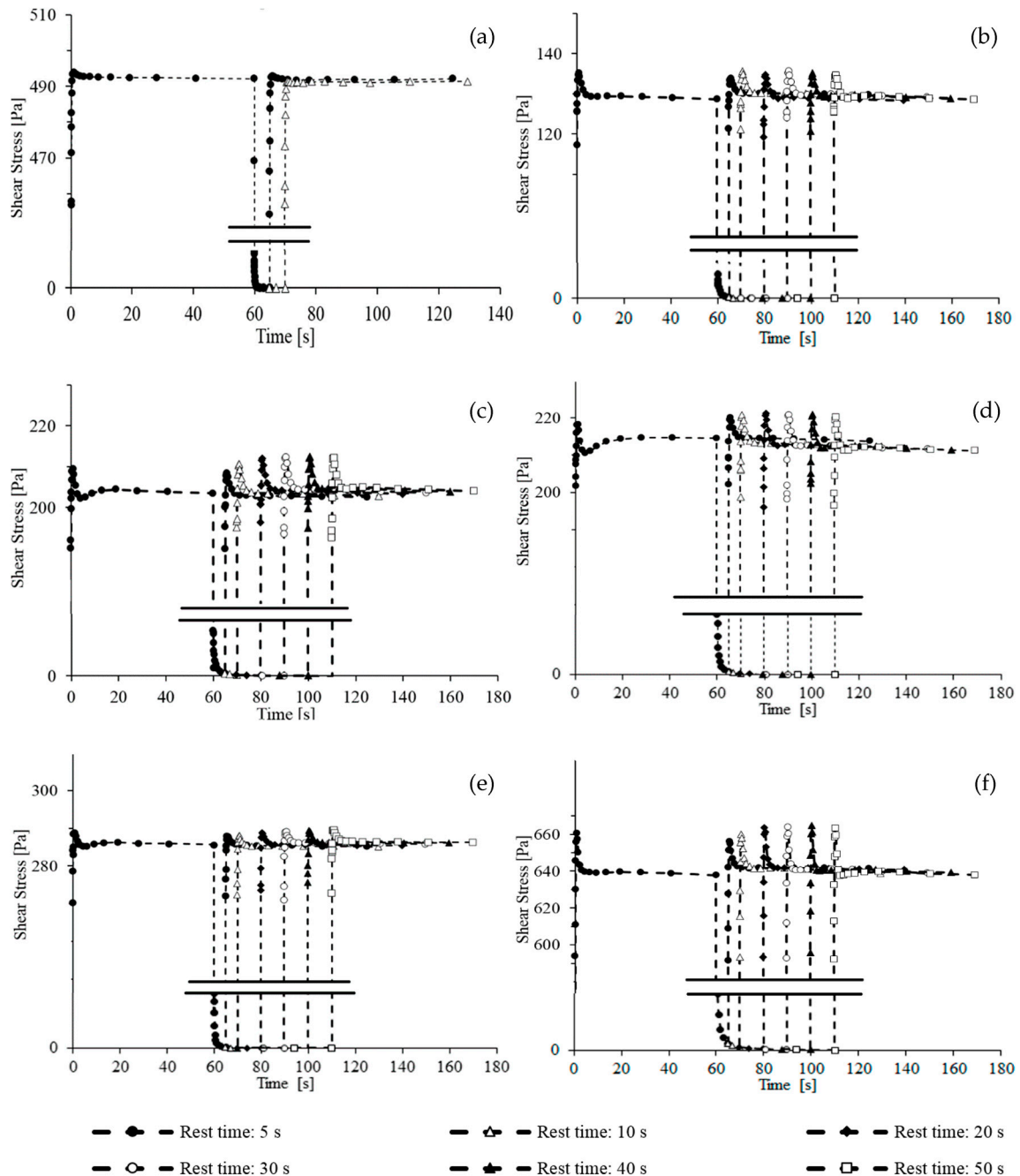
### 3.2.5. Interrupted Shear Flow

Figure 5a–f shows the stress growth upon the interrupted shear flow of: (a) The original asphalt, (b) AR-BGR25-10LP, (c) AR-BGR50-15LP, (d) AR-BGR50-20LP, (e) AR-BGR75-10LP, and (f) AR-BGR75-20LP ( $T = 64\text{ }^\circ\text{C}$ , rest times of 5, 10, 20, 30, 40, and 50 s, as well as a shear rate of  $2\text{ s}^{-1}$ ).

Literature has shown that the conventional asphalt has no peak overshoot of shear stress, just a steady-state shear flow, and rapid stress relaxation as complied with the original asphalt, as can be seen in Figure 5a [36]. Wekumbura et al. reported that “This type of behavior must be due to the weak associations, e.g., bipolar attractions, hydrogen bonding etc., which are easily destroyed by stressing or temperature variations [36].” This differs with binders modified with polymer components associated with peak overshoots [36,37].

Overall, asphalt–rubber–guayule binders had the potential to get back to its original peak overshoot very fast through the first 50 s, the maximum after releasing the original shear growth—both initial and second overshoots followed by steady-state shear stress. The effect of asphalt, rubber, and guayule resin concentrations appeared here on the resultant stress growth of each asphalt–rubber–guayule binder. For instance, AR-BGR75-20LP had an initial overshoot of about 660 Pa. Even though a 5 s period was sufficient for flow relaxation, the second stress growth (655 Pa) did not reach the initial

value. However, a 10 s rest time was sufficient to yield a fully recovered overshoot. This binder achieved about 1.34 times the original asphalt according to its original overshoot and about 1.3 times according to the steady-state value. This reflects a better performance of AR-BGR75-20LP in this regard. On the other hand, all other asphalt–rubber–guayule binders resulted in observed peak overshoots, as shown in Figure 5b–e, but their stress growth patterns were lower than the one attributed to the original asphalt.



**Figure 5.** Stress growth in the interrupted shear flow of (a) the original asphalt (PG64-22), (b) AR-BGR25-10LP, (c) AR-BGR50-15LP, (d) AR-BGR50-20LP, (e) AR-BGR75-10LP, and (f) AR-BGR75-20LP.  $T = 64\text{ }^{\circ}\text{C}$  and a shear rate of  $2\text{ s}^{-1}$ .

The concept of the interrupted shear flow test applied in this paper complied with the literature [19,29,36,37]. The results showed a positive impact of polymeric components dissolved in the liquid asphalt–rubber–guayule binder, as they created a peak overshoot of shear stress in addition to its distinct rapid recovery time when applying the second stress growth. Ultimately, the authors can claim that the polymeric components dissolved from the CRM in the asphalt–rubber–guayule binder resulted in a 3D network structure that indicates an improvement against the conventional asphalt binder.

### 3.2.6. CRM Dissolution: Asphalt–Rubber–Guayule Binders vs. Corresponding Asphalt–Rubber Binders

Figure 6 depicts the dissolved CRM% in a comparison between the asphalt–rubber–guayule binders and their corresponding asphalt–rubber binders. There was no clear evidence that the CRM was more dissolved in the asphalt–rubber binder than asphalt–rubber–guayule binders and vice versa. It could be declared that there was no significant difference between asphalt–rubber–guayule binders and their corresponding asphalt–rubber binders regarding their CRM dissolution average, 29% and 30%, respectively. Nevertheless, the standard deviation for the asphalt–rubber–guayule binder was higher than that of the corresponding asphalt–rubber binders—8.9 and 3.4, respectively—indicating the variable influence of different proportions of guayule resin in the asphalt–rubber–guayule binders.

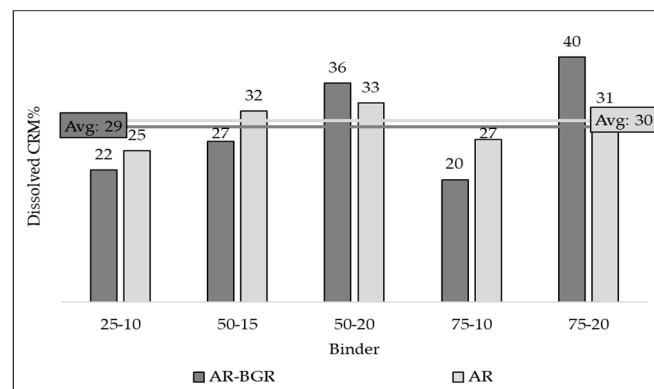


**Figure 6.** Crumb rubber modifier (CRM) dissolution: Asphalt–rubber–guayule binders vs. asphalt–rubber binders.

## 3.3. TGA

### 3.3.1. TGA of Guayule Resin

Guayule resin, as a new material, was exposed to compositional analysis via TGA to indicate its multi-components. However, a detailed study regarding these constituents was out of the scope of this research. Figure 7 shows the complexity of guayule resin multi-components that contained constituents that decomposed at 233, 262, 286, 313, 339, 341, 366, 391, and 418 °C, upon the decomposition temperature range from the ambient temperature to 450 °C, which corresponded to almost no residue. The 450 °C terminal temperature was first determined by the ramp method as a rapid approach to recognize a 100% decomposition of the guayule resin material. Nevertheless, SITG was utilized to define the decomposition temperatures of guayule resin constituents because it prevents the overlapping of the decomposition temperatures of components in addition to rendering a high accuracy compared to the ramp method [22].

The very low molecular weight components were gradually lost in a decomposition temperature ranged from the ambient temperature to 233 °C, resulting in a mass loss of 3.4%, as can be seen in Figure 8. The tested specimen was heat-treated for 4 h, 600 rpm, and 160 °C interaction parameters. On the other hand, the as-received guayule resin was thermally analyzed. As can be seen in Figure 8a, the minimum point at 100 °C on DTG corresponds to about a 0.82% moisture mass loss indicating a

small amount of moisture. However, when the guayule resin was heat-treated, the DTG did not show the minimum point at 100 °C, indicating no moisture at this condition. Additionally, the mass loss was determined to be 0.14% at 100 °C, as shown in Figure 8b, which may represent a partial loss of very low molecular weight components of guayule resin.

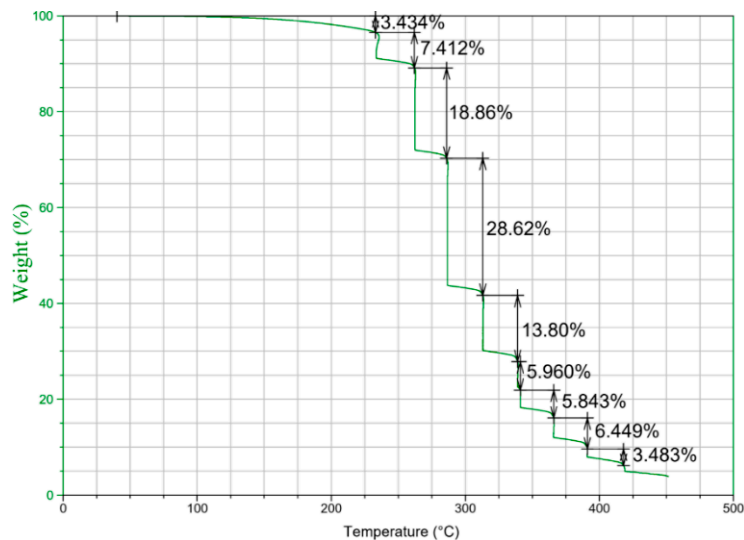


**Figure 7.** Thermo-gravimetric analysis (TGA) chart of 4 h heat-treated guayule resin (B(4)), stepwise isothermal thermo-gravimetric (SITG) method—from ambient temperature to 450 °C.

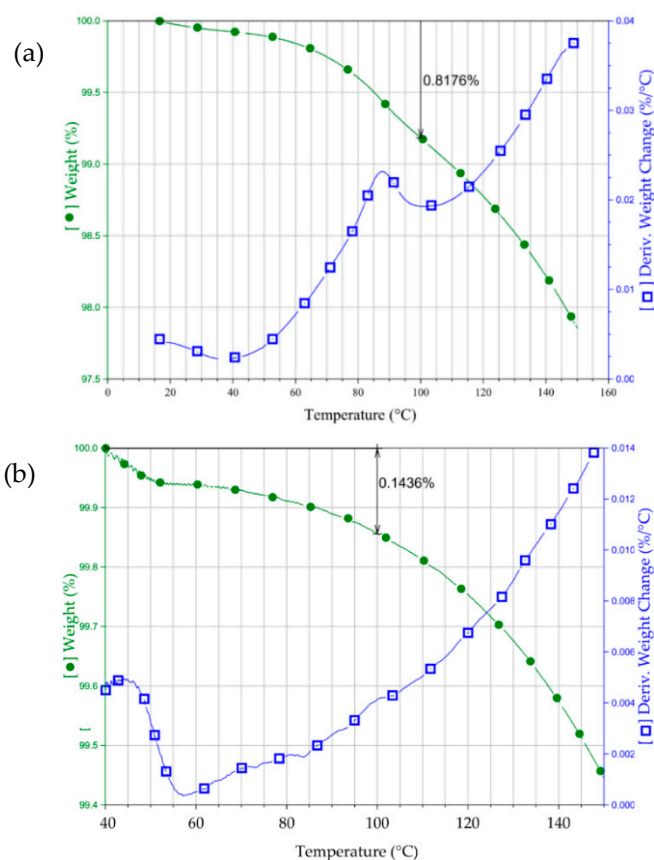


**Figure 8.** Moisture investigation of guayule resin by TGA: (a) As-received material, and (b) after 4 h heat treatment at 160 °C, and 600 rpm.

### 3.3.2. TGA Analysis of CRM

#### a. As-Received CRM

The TGA charts and DTGs of as received and extracted CRMs from asphalt–rubber–guayule binders were studied. However, for brevity, TGA charts, and DTGs of the as-received CRM are presented in Figure 9. As can be seen in Figure 9, the CRM decomposition was represented by the mass loss, which was 6.2% for oily components, 36.8% for natural rubber, 17.2% for synthetic rubber, and 39.9% for filler components.

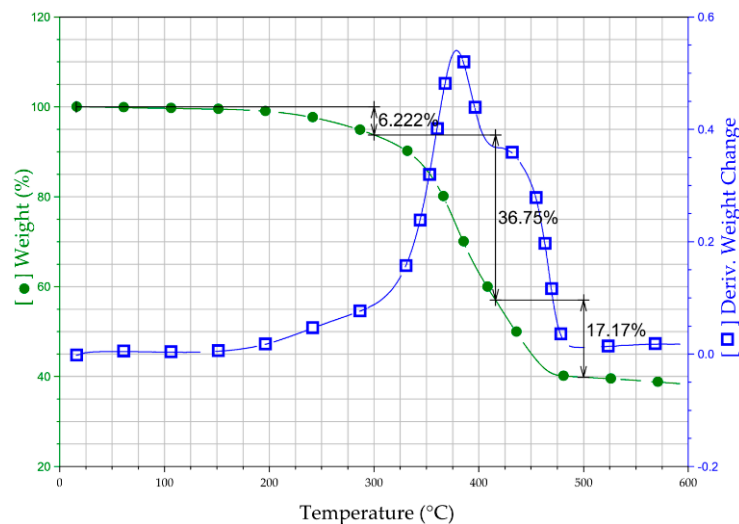


**Figure 9.** TGA chart and derivative thermo-gravimetric (DTG) of the as-received CRM.

#### b. Extracted CRM

The CRM was released from the binder liquid phase, as mentioned above. Consecutively, the dissolved CRM was calculated for the binder whole matrix. As can be seen in Figure 10, the higher CRM dissolution resulted in a higher CRM concentration such as 40.5% and 36.2% for AR-BGR75-20 and AR-BGR50-20, respectively. Nevertheless, this went lower with lower CRM concentration, such as in the case of AR-BGR50-15 and AR-BGR75-10 that resulted in a dissolved CRM percentage of 26.6% and 20.3%, respectively. Furthermore, AR-BGR25-10 yielded 21.8% dissolved CRM. As the CRM dissolution analysis indicated a maximum of about 40% of dissolved CRM that could not justify the close pass/fail temperatures of the liquid phase vs. the whole matrix, as shown in Table 4.

As shown in Figure 10, the TGA outcomes were translated as concentrations of CRM constituents, including the dissolved portion and the extracted portion. The latter was studied to expose the changes in the four major components of the extracted CRM. This was carried out for the as-received CRM and the CRM extracted from the five asphalt–rubber–guayule binders. The extracted CRM constituents indicated relatively little dissolution of fillers (about 14% release on average). The dissolution of the polymeric components (natural rubber and synthetic rubber) was about 41% and 25% on average, respectively. However, a significant dissolution took place to the oily components, about 67% on average.

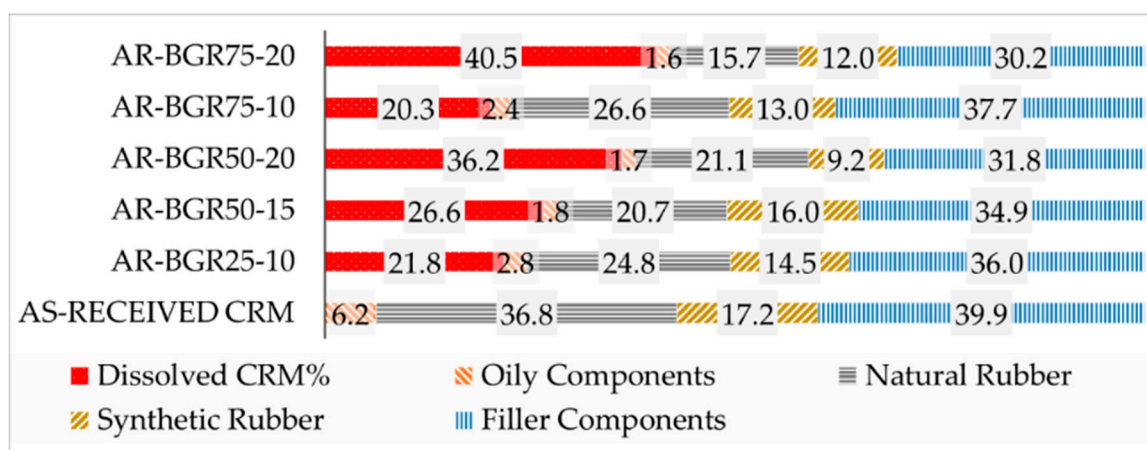


**Figure 10.** Four major components of the extracted CRM and the dissolved amount in binder regarding the five selected binders and the as-received CRM.

#### 4. Conclusions

This study aimed to investigate the potential of replacing a large portion of the original asphalt (PG64) by guayule resin (PG52) to compensate for the original asphalt behavior at high temperatures. Attempts of different proportions of asphalt and guayule in addition to the CRM as an enhancer were made. Furthermore, investigations related to their corresponding asphalt–rubber binders were presented. Since the CRM modified binder did not always perform as a whole matrix, the binder liquid phase (worst case scenario) was investigated for selected binders. Per study limitations, the authors found that the optimum blend, which was 62.5% asphalt, 12.5% rubber, and 25% guayule resin, provided better performance than that of the original asphalt in all studied scales, whether as a whole matrix or a liquid phase. However, as expected, the corresponding asphalt–rubber binder resulted in relatively higher performance.

The study showed asphalt guayule compatibility (or homogeneity) with no phase separation or guayule resin coagulation. Pure guayule resin presented unconventional master-curve trends, which provided better behavior than original asphalt at low frequencies in terms of  $G'$ ,  $G''$ , and  $\delta$ . Accordingly, this might be beneficial in low-speed applications. It also presented an unconventional  $\delta$  trend with the frequency sweep opposite to the original asphalt trend. This  $\delta$  trend was desired in the asphalt industry, as it provided higher elastic behavior at lower traffic speeds. Consecutively, one may notice that asphalt–rubber–guayule binders provided better master-curve trends at lower frequencies (Figure 3). With the study limitations, a formation of a 3D network structure was proven for asphalt–rubber–guayule binders, thus reflecting the release of the CRM polymeric components in the binder liquid phase as verified by TGA—proven to yield better performance in literature. Ultimately, this kind of research may provide future solutions in the asphalt industry in terms of sustainability, economics, and environmental concerns.

**Author Contributions:** The authors confirm contribution to the paper as follows: Conceptualization, M.A. and A.H.; methodology, M.A. and A.H.; data collection and lab testing, A.H.; validation, M.A. and A.H.; formal analysis, A.H. and M.A.; investigation, A.H. and M.A.; writing—original draft preparation, A.H. and M.A.; writing—review and editing, M.A. and A.H.; visualization, M.A.; supervision, M.A.; and project administration, M.A.

**Funding:** This research was funded by Missouri University of Science and Technology.

**Acknowledgments:** We would like to show our gratitude to Bridgestone Americas for creating guayule resin that we worked on in addition to their assistance for the information we requested. Likewise, we would like to thank Steven Lusher, for assistance with providing the material samples and information we requested upon his experience with guayule.

**Conflicts of Interest:** The authors declare no conflict of interest.

## References

1. Nakayama, F. Guayule future development. *Ind. Crop. Prod.* **2005**, *22*, 3–13. [CrossRef]
2. Tullo, A.H. Guayule gets ready to hit the road. *Chem. Eng. News* **2015**, *93*, 18–19.
3. Schloman, W.W., Jr.; Garrot, D.J., Jr.; Ray, D.T.; Bennett, D.J. Seasonal effects on guayule resin composition. *J. Agric. Food Chem.* **1986**, *34*, 177–179. [CrossRef]
4. Costa, E.; Aguado, J.; Ovejero, G.; Cañizares, P. Conversion of guayule resin to C1–C10 hydrocarbons on zeolite based catalysts. *Fuel* **1992**, *71*, 109–113. [CrossRef]
5. Gumbs, R.W. Guayule Resin Multipolymer. Patent EP2205679A1, 16 April 2009.
6. Lusher, S.M. Guayule Plant Extracts as Binder Modifiers in Flexible (Asphalt) Pavement Mixtures. Ph.D. Thesis, Missouri University of Science and Technology, Rolla, MO, USA, 2018.
7. Schloman, W.W., Jr.; Hively, R.A.; Krishen, A.; Andrews, A.M. Guayule byproduct evaluation: Extract characterization. *J. Agric. Food Chem.* **1983**, *31*, 873–876. [CrossRef]
8. Richardson, D.N.; Lusher, S.M. *The Guayule Plant: A Renewable, Domestic Source of Binder Materials for Flexible Pavement Mixtures*; Transportation Research Board: Washington, DC, USA, 2013.
9. Hemida, A.; Abdelrahman, M. A Threshold to Utilize Guayule Resin as a New Binder in Flexible Pavement Industry. *Int. J. Eng. Res. Appl.* **2018**, *8*, 83–94.
10. Wright, N.; Fansler, S.; Lacewell, R. *Guayule Economics. Guayule Natural Rubber*; Office of Arid Lands Studies: Tucson, AZ, USA, 1991; pp. 351–365.
11. Zaumanis, M.; Mallick, R.B.; Frank, R. 100% recycled hot mix asphalt: A review and analysis. *Resour. Conserv. Recycl.* **2014**, *92*, 230–245. [CrossRef]
12. Riddell, A.; Ronson, S.; Counts, G.; Spenser, K. Towards Sustainable Energy: The Current Fossil Fuel Problem and the Prospects of Geothermal and Nuclear Power. Available online: [http://web.stanford.edu/class/e297c/trade\\_environment/energy/hfossil.html](http://web.stanford.edu/class/e297c/trade_environment/energy/hfossil.html) (accessed on 25 May 2019).
13. Asphalt and Fuel Index: Asphalt Cement Price Index. Available online: <http://www.dot.ga.gov/PS/Materials/AsphaltFuelIndex> (accessed on 25 May 2019).
14. Putman, B.J.; Amirhanian, S.N. Characterization of the Interaction Effect of Crumb Rubber Modified Binders Using HP-GPC. *J. Mater. Civ. Eng.* **2010**, *22*, 153–159. [CrossRef]
15. Ragab, M. *Enhancing the Performance of Crumb Rubber Modified Asphalt through Controlling the Internal Network Structure Developed*; North Dakota State University: Fargo, ND, USA, 2016.
16. Ghavibazoo, A.; Abdelrahman, M.; Ragab, M. Mechanism of Crumb Rubber Modifier Dissolution into Asphalt Matrix and Its Effect on Final Physical Properties of Crumb Rubber–Modified Binder. *Transp. Res. Rec. J. Transp. Res. Board* **2013**, *2370*, 92–101. [CrossRef]
17. Ragab, M.; Abdelrahman, M.; Ghavibazoo, A. New Approach for Selecting Crumb-Rubber-Modified Asphalts for Rutting and Permanent Deformation Resistance. *Adv. Civ. Eng. Mater.* **2013**, *2*, 360–378. [CrossRef]
18. Zanzotto, L.; Kennepohl, G. Development of Rubber and Asphalt Binders by Depolymerization and Devulcanization of Scrap Tires in Asphalt. *Transp. Res. Rec. J. Transp. Res. Board* **1996**, *1530*, 51–58. [CrossRef]
19. Ragab, M.; Abdelrahman, M.; Ghavibazoo, A. Performance Enhancement of Crumb Rubber–Modified Asphalts through Control of the Developed Internal Network Structure. *Transp. Res. Rec. J. Transp. Res. Board* **2013**, *2371*, 96–104. [CrossRef]
20. Ghavibazoo, A.; Abdelrahman, M. Composition analysis of crumb rubber during interaction with asphalt and effect on properties of binder. *Int. J. Pavement Eng.* **2013**, *14*, 517–530. [CrossRef]
21. Attia, M.; Abdelrahman, M. Enhancing the performance of crumb rubber-modified binders through varying the interaction conditions. *Int. J. Pavement Eng.* **2009**, *10*, 423–434. [CrossRef]
22. Ghavibazoo, A.; Abdelrahman, M.; Ragab, M. Effect of Crumb Rubber Modifier Dissolution on Storage Stability of Crumb Rubber–Modified Asphalt. *Transp. Res. Rec. J. Transp. Res. Board* **2013**, *2370*, 109–115. [CrossRef]
23. Ghavibazoo, A.; Abdelrahman, M.; Ragab, M. Changes in composition and molecular structure of asphalt in mixing with crumb rubber modifier. *Road Mater. Pavement Des.* **2016**, *17*, 906–919. [CrossRef]
24. Ghavibazoo, A.; Abdelrahman, M. Effect of Crumb Rubber Dissolution on Low-Temperature Performance and Aging of Asphalt–Rubber Binder. *Transp. Res. Rec. J. Transp. Res. Board* **2014**, *2445*, 47–55. [CrossRef]
25. Abdelrahman, M.; Katti, D.R.; Ghavibazoo, A.; Upadhyay, H.B.; Katti, K.S. Engineering Physical Properties of Asphalt Binders through Nanoclay–Asphalt Interactions. *J. Mater. Civ. Eng.* **2014**, *26*, 4014099. [CrossRef]

26. ASTM. *ASTM D2042-15, Standard Test Method for Solubility of Asphalt Materials in Trichloroethylene*; ASTM International: West Conshohocken, PA, USA, 2015.
27. AASHTO. *AASHTO T44-13, Standard Method of Test for Solubility of Bituminous Material*; American Association of State Highway Transportation Officials (AASHTO): Washington, DC, USA, 2013.
28. ASTM. *ASTM D7173-14, Standard Practice for Determining the Separation Tendency of Polymer from Polymer Modified Asphalt*; ASTM International: West Conshohocken, PA, USA, 2014.
29. Ragab, M.; Abdelrahman, M. Enhancing the crumb rubber modified asphalt's storage stability through the control of its internal network structure. *Int. J. Pavement Res. Technol.* **2018**, *11*, 13–27. [[CrossRef](#)]
30. Hansen, C.M. 50 Years with solubility parameters—Past and future. *Prog. Org. Coat.* **2004**, *51*, 77–84. [[CrossRef](#)]
31. Zhang, C.; Kessler, M.R. Bio-based Polyurethane Foam Made from Compatible Blends of Vegetable-Oil-Based Polyol and Petroleum-Based Polyol. *ACS Sustain. Chem. Eng.* **2015**, *3*, 743–749. [[CrossRef](#)]
32. Zhao, G.; Ni, H.; Ren, S.; Fang, G. Correlation between Solubility Parameters and Properties of Alkali Lignin/PVA Composites. *Polymers* **2018**, *10*, 290. [[CrossRef](#)]
33. Duong, D.T.; Walker, B.; Kim, C.; Purushothaman, B.; Nguyen, T.-Q.; Lin, J.; Love, J.; Anthony, J.E.; Nguyen, T. Molecular solubility and hansen solubility parameters for the analysis of phase separation in bulk heterojunctions. *J. Polym. Sci. Part B Polym. Phys.* **2012**, *50*, 1405–1413. [[CrossRef](#)]
34. Hansen, C.M. *Solubility Parameters: A User's Handbook*; CRC Press: Boca Raton, FL, USA, 2007.
35. AASHTO. *AASHTO T315-12, Standard Method of Test for Determining the Rheological Properties of Asphalt Binder Using a Dynamic Shear Rheometer (DSR)*; American Association of State Highway Transportation Officials (AASHTO): Washington, DC, USA, 2013.
36. Wekumbura, C.; Stastna, J.; Zanzotto, L. Destruction and Recovery of Internal Structure in Polymer-Modified Asphalts. *J. Mater. Civ. Eng.* **2007**, *19*, 227–232. [[CrossRef](#)]
37. Jasso, M.; Bakoš, D.; Stastna, J.; Zanzotto, L. Conventional asphalt modified by physical mixtures of linear SBS and montmorillonite. *Appl. Clay Sci.* **2012**, *70*, 37–44. [[CrossRef](#)]
38. Shen, J.; Amirkhani, S. The influence of crumb rubber modifier (CRM) microstructures on the high temperature properties of CRM binders. *Int. J. Pavement Eng.* **2005**, *6*, 265–271. [[CrossRef](#)]
39. Lee, S.-J.; Amirkhani, S.N.; Shatanawi, K.; Kim, K.W. Short-term aging characterization of asphalt binders using gel permeation chromatography and selected Superpave binder tests. *Constr. Build. Mater.* **2008**, *22*, 2220–2227. [[CrossRef](#)]
40. Diab, A.; You, Z. Small and large strain rheological characterizations of polymer- and crumb rubber-modified asphalt binders. *Constr. Build. Mater.* **2017**, *144*, 168–177. [[CrossRef](#)]
41. Ghavibazoo, A.; Abdelrahman, M. Monitoring Changes in Composition of Crumb Rubber Modifier During Interaction with Asphalt and Its Effect on Final Modified Asphalt Performance. In Proceedings of the 91st Annual Meeting of the Transportation Research Board, Washington, DC, USA, 22–26 January 2012.
42. Parkes, G.M.B.; Barnes, P.A.; Charsley, E.L. New Concepts in Sample Controlled Thermal Analysis: Resolution in the Time and Temperature Domains. *Anal. Chem.* **1999**, *71*, 2482–2487. [[CrossRef](#)]

